14th World Congress on Computational Mechanics (WCCM)
ECCOMAS Congress 2020)
Virtual Congress: 11-–15 January 2021
F. Chinesta, R. Abgrall, O. Allix and M. Kaliske (Eds)

A COMPARATIVE STUDY OF NUMERICAL SIMULATION STRATEGIES IN INJECTION MOLDING

DENIS ANDERS[1], MARKUS BAUM[2] AND JOHANNES ALKEN[1]

[1] Cologne University of Applied Sciences (TH Köln)
Group for Computational Mechanics and Fluid Dynamics
Steinmüllerallee 1, 51643 Gummersbach, Germany,
E-Mail: denis.anders@th-koeln.de

[2] Cologne University of Applied Sciences (TH Köln)
Group for Computational Mechanics and Fluid Dynamics
Steinmüllerallee 1, 51643 Gummersbach, Germany,
E-Mail: markus.baum@th-koeln.de

[3] Cologne University of Applied Sciences (TH Köln)
Group for Computational Mechanics and Fluid Dynamics
Steinmüllerallee 1, 51643 Gummersbach, Germany,
E-Mail: johannes.alken@th-koeln.de

Key words: Injection Molding, Computational Fluid Dynamics, Hele-Shaw Approximation, Computing Methods, Polymers

Abstract. Injection molding is undoubtedly one of the most widely used manufacturing process for polymers [1]. Due to its advantages over other processing techniques in terms of good surface finish, the ability to process complex parts without the need of secondary operations and low cost for mass production, injection molding has found its way into various branches of industry [2]. In order to implement process optimization a thorough understanding of the material behaviour, the filling process as well as the underlying physical phenomena is necessary. A suitable way to address this issue is the application of numerical simulation of the injection molding process. In this contribution the authors present a comparative numerical study for the mold filling of an exemplary thin-walled mold geometry. For the numerical simulation the commercial CFD software packages Cadmould 3D-F and ANSYS CFX are employed. Both software packages make use of different simulation strategies. In ANSYS CFX a three-dimensional classical CFD approach is employed for the mold filling which is of course very accurate but extremely time consuming. Cadmould 3D-F pursues a generalized Hele–Shaw approximation (also known as so-called 2,5-D approach) which is due to some simplifying assumptions less accurate but also much less costly in terms of computing time [2, 5].

1 INTRODUCTION

Over the past 30 years, injection molding (IM) has seen a rapid technological development and opened up new fields of application for electronic components devices, medical devices as well as in the automotive/transport industry and packaging industry. In the field of primary forming processes, it is one of

the most important manufacturing processes in the plastics processing industry, alongside extrusion. The advancing globalization of the markets for plastic products is leading to increased demands on process efficiency and product quality. In this context, the typical requirements are

- mass homogeneity and high dimensional accuracy
- minimization of shrinkage and warpage
- surface structure (degree of gloss and the surface quality)
- strength properties (e.g. fibre orientation for glass fibre reinforced plastics)

Optimization of product quality while minimizing process costs requires companies to have an in-depth understanding of the injection molding process. Here, injection molding simulation plays a crucial role. The aim is to determine the influence of adjustable process variables such as mould cavity characteristics, gating and temperature control system, volume flow, process pressure and temperatures, etc. on the relevant quality indicators like cycle time, dimensional accuracy, shrinkage/distortion, energy consumption, etc. The results of the simulation consequently serve as a basis for subsequent iterative optimization of the process using statistical methods of data analysis, e.g. design of experiment (DOE), artificial neural network (ANN), machine learning techniques (ML), etc. The basic scheme of this iterative optimization process is illustrated in figure 1.

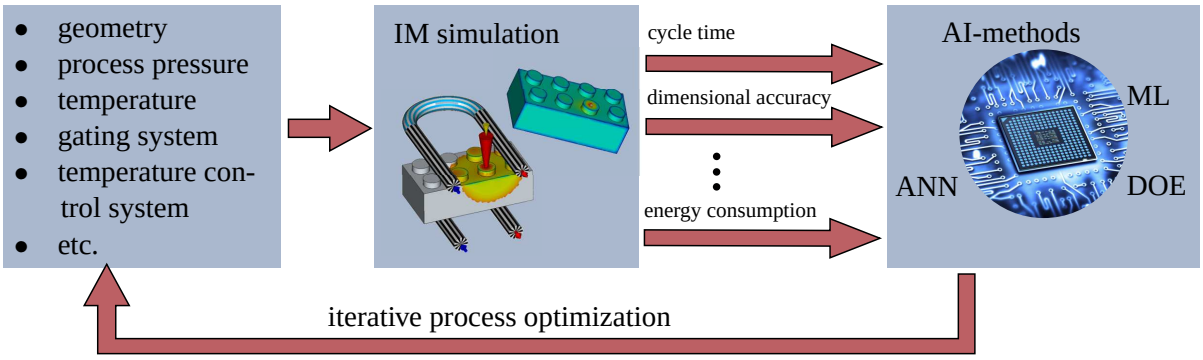

Figure 1: Scheme of the iterative optimization process in injection molding.

2 FUNDAMENTALS AND MATHEMATICAL MODELLING OF THE INJECTION MOLDING PROCESS

In order to get a better understanding of this contribution and the relevance of the research topic, the authors provide a concise introduction into some fundamentals and basic principles of the injection molding process as well as the corresponding mathematical background.

2.1 Fundamentals of the injection molding process

In injection molding, the polymer, which is located in a plasticizing unit and heated to melting temperature, is injected at high pressure into the cavity of a mold, cf. figure 2. There, the polymer is first compressed due to its compressibility before it cools and solidifies. As soon as sufficient stiffness is reached to allow for demoulding, the mold is opened and the injection-moulded part is ejected.

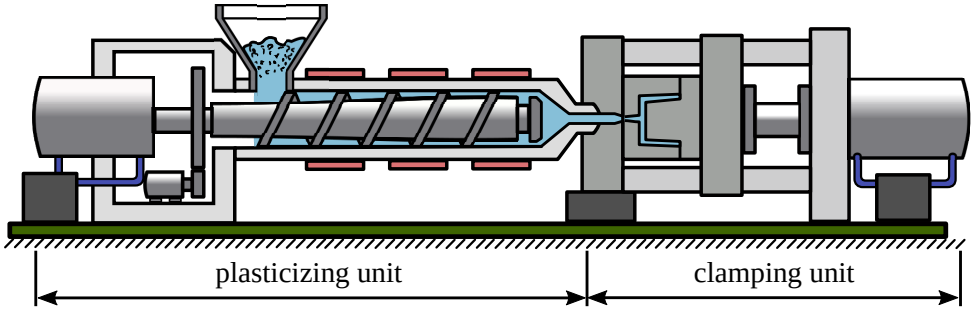

Figure 2: Illustration of an injection molding machine with plasticizing and clamping unit.

The main advantages of the injection moulding process can be summarized as follows:

- fully automated and extremely fast production process,
- cost-effective production of complex molded parts in large quantities,
- further finishing of the molded parts is usually not necessary.

The essential disadvantages of the injection molding process are the relatively high manufacturing costs for the molds compared to the actual process. For this reason, subsequent modifications to the mold are extremely expensive and need to be prevented by thorough numerical investigations in the early stages of product design as well as the cooling strategy.
Due to the process characteristics there are some special challenges in injection molding such as

- component optimization and process-compatible design
- adjustment of an accurate or low-error filling characteristic
- process control close to the optimum operating point
- optimization of gating systems for balanced filling of single and multiple cavities
- design of a suitable temperature control layout for the injection mold

In the context of this contribution, special emphasis is put on the filling phase, as this has a significant influence on the product quality. As shown in figure 3, different thickness distributions can lead to filling problems like weld lines or air inclusions due to inhomogeneous flow resistances. A balanced filling process avoiding filling problems is especially for complex geometries as well as for multiple cavities a very demanding task. For this end, numerical filling studies are employed in the early stages of product development.

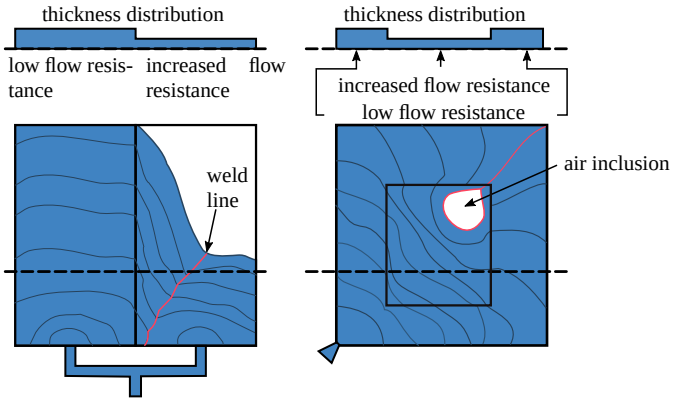

Figure 3: Effects of different flow resistances on the filling process due to thickness changes.

The filling process has also a strong effect on the heat transfer within the cavity, as illustrated in figure 4. Inhomogeneous filling conditions due to different flow velocities and shear stresses within the cavity usually induce inhomogeneous heat transfer conditions. This finally can cause strongly pronounced geometric distortion as well as shrinkage and warpage.

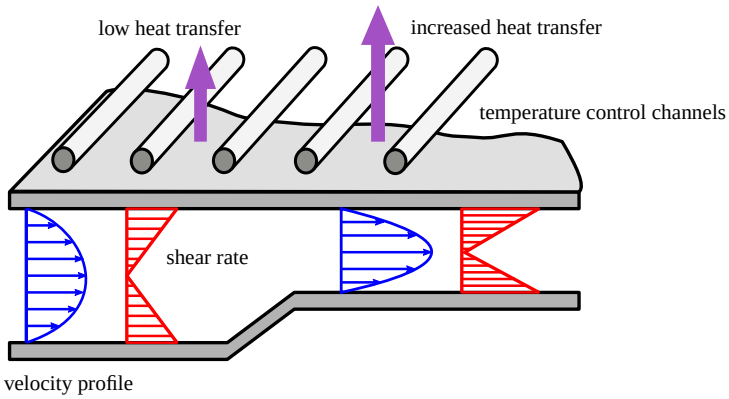

Figure 4: Effects of thickness changes on heat transfer in the mold cavity.

2.2 Mathematical modelling of the injection molding process

There are two main approaches within the context of modelling the injection molding process – a volumetric and a semi-volumetric approach, respectively. In the fully volumetric 3D modelling of the cavity, the volume is spatially discretized by using the classical finite volume method and the fully Navier-Stokes equations as governing equations [6, 7, 8]. In the semi-volumetric framework, so-called 2,5D modelling approaches are employed. The volumetric model is replaced by a suitable mid-plane or surface model [9]. The surfaces are transformed into a 2D finite element mesh and the volume is discretized via networks of bar elements [5]. These different discretization strategies according to [3] are illustrated in figure 5.

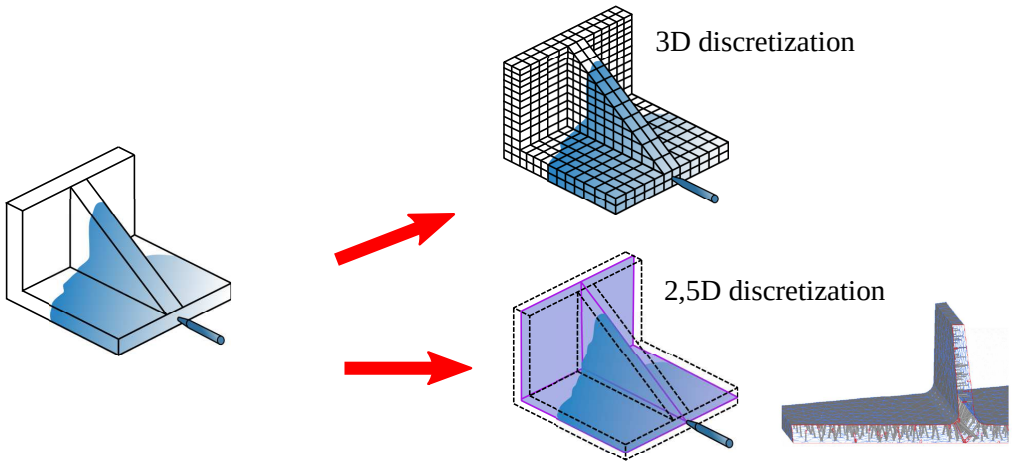

Figure 5: Comparison of 3D and 2,5D modelling approaches.

In the 3D modelling, the complete Navier-Stokes equations including the mass balance are considered

during the filling phase:

$$\begin{aligned} \frac{\partial \rho}{\partial t} + \nabla \cdot (\rho \vec{u}) &= 0 \\ \frac{\partial}{\partial t}(\rho \vec{u}) + \nabla \cdot (\rho \vec{u} \otimes \vec{u} - \sigma) &= \rho \vec{g} \\ \sigma = -p \cdot I + \eta \left(\nabla \vec{u} + \nabla \vec{u}^T \right) & \end{aligned} \tag{1}$$

For the thermal analysis the above equations are coupled with the energy balance

$$\rho c_p \left(\frac{\partial T}{\partial t} + \vec{u} \cdot \nabla T \right) = \nabla \cdot (\lambda \nabla T) + \eta \dot{\gamma}^2. \tag{2}$$

In the scope of 2,5D modelling, a generalized Hele-Shaw approximation of the Navier-Stokes equations is used for the filling phase [10]:

$$\begin{aligned} \frac{\partial \rho}{\partial t} + \frac{\partial}{\partial x}(\rho u_x) + \frac{\partial}{\partial y}(\rho u_y) &= 0 \\ \frac{\partial p}{\partial x} &= \frac{\partial}{\partial z}\left(\eta \frac{\partial u_x}{\partial z} \right) \\ \frac{\partial p}{\partial y} &= \frac{\partial}{\partial z}\left(\eta \frac{\partial u_y}{\partial z} \right) \end{aligned} \tag{3}$$

The Hele-Shaw approximation is motivated by the usually small wall thickness of injection molded components [11]. The associated energy balance is simplified in this formulation to

$$\rho c_p \left(\frac{\partial T}{\partial t} + u_x \frac{\partial T}{\partial x} + u_y \frac{\partial T}{\partial y} \right) = \lambda \frac{\partial^2 T}{\partial z} + \eta \dot{\gamma}^2 \quad \text{with} \quad \dot{\gamma} = \sqrt{\left(\frac{\partial u_x}{\partial z} \right)^2 + \left(\frac{\partial u_y}{\partial z} \right)^2}. \tag{4}$$

Within these equations, the *z*-coordinate characterizes the thickness direction within of the melt.

Polymer melts generally have a shear thinning (pseudo-plastic) behaviour and thus belong to the non-Newtonian fluids. Their viscosity therefore depends on the shear rate $\dot{\gamma}$. Formally, it applies $\eta = f(\dot{\gamma}, T, p)$.
Various models have been developed for the mathematical description of viscosity behaviour. The most common viscosity models in injection molding simulation are the Cross-WLF model and the Carreau-WLF model, cf. [4]. The viscosity in the Cross-WLF model is given by

$$\eta(\dot{\gamma}, T, p) = \frac{\eta_0(T, p)}{1 + \left(\frac{\eta_0(T, p)\dot{\gamma}}{\tau^*} \right)^{1-n}}. \tag{5}$$

Here η_0 denotes the reference viscosity, τ^* is the critical shear stress at the transition to non-Newtonian behavior and *n* characterizes the power profile at high shear rate. The reference viscosity follows from the WLF approach by

$$\eta_0(T, p) = D_1 \cdot \exp\left[\frac{-A_1 (T - D_2 - D_3 \cdot p)}{\widetilde{A}_2 + T - D_2} \right]. \tag{6}$$

In the Carreau-WLF model the viscosity is determined according to [12]

$$\eta\left(\dot{\gamma},T,p\right)=\frac{a_{\mathrm{T}}\left(T,p\right)\cdot A}{\left(1+a_{\mathrm{T}}\left(T,p\right)\cdot B\cdot\dot{\gamma}\right)^{C}}. \tag{7}$$

Here a_{T} denotes the temperature shift factor, A is the reference viscosity, B the reciprocal transition velocity and c the slope of the viscosity curve in the pseudo-plastic viscosity range for $\dot{\gamma}\to\infty$. The temperature shift factor follows from the WLF equation [12, 13]

$$\lg\left(a_{\mathrm{T}}\right)=\frac{C_1\left(T_0-T_S\right)}{C_2+\left(T_0-T_S\right)}-\frac{C_1\left(T-T_S\right)}{C_2+\left(T-T_S\right)}. \tag{8}$$

In the holding-pressure phase the cavity is completely filled with the polymer melt. For the compensation of thermal shrinkage, further polymer melt is pressed into the cavity due to its compressibility. In order to adequately describe this behavior a model for the consideration of compressibility is required. For the modelling of the equation of state (pvT-relationship) there are several approaches, e.g. Spencer-Gilmore or Tait model [2, 14]. For the simulation of amorphous polymers the modified Tait model is usually used:

$$v\left(p,T\right)=v\left(0,T\right)\left[1-C\cdot\ln\left(1+\frac{p}{B\left(T\right)}\right)\right]+v_t\left(p,T\right),\ \text{with}\ C=0{,}0894 \tag{9}$$

$$v\left(0,T\right)=\begin{cases}b_{1m}+b_{2m}\left(T-b_5\right), & T>T_t\\ b_{1s}+b_{2s}\left(T-b_5\right), & T<T_t\end{cases},\quad B\left(T\right)=\begin{cases}b_{3m}e^{-b_{4m}\left(T-b_5\right)}, & T>T_t\\ b_{3s}e^{-b_{4s}\left(T-b_5\right)}, & T<T_t\end{cases} \tag{10}$$

$$v_t\left(p,T\right)=\begin{cases}0, & T>T_t\\ b_7e^{b_8\left(T-b_5\right)-b_9p}, & T<T_t\end{cases} \tag{11}$$

Here $T_t\left(p\right)=b_5+b_6p$ is the transition temperature between solid and liquid state [2]. The parameters $b_\bullet$ are fitting parameters of the model. For the simulation of semi-crystalline polymers the parameter $v_t(p,T)$ is zero [15].

For the calculation of shrinkage and warpage it is necessary to determine the residual stresses of the component. These stresses result mainly from inhomogeneous cooling and thermally induced shrinkage of the molded part. The underlying viscoelastic material behaviour is modelled by a corresponding anisotropic linear thermo-viscoelastic model [16]:

$$\sigma_{ij}=\int_0^t C_{ijkl}\left(\xi\left(t\right)-\xi\left(t'\right)\right)\cdot\left(\frac{\partial\varepsilon_{kl}}{\partial t'}-\alpha_{th,kl}\frac{\partial T}{\partial t'}\right)\mathrm{d}t'$$

where σ_{ij} and ε_{kl} are the stress and strain tensors, respectively [3]. The stresses within the molded part thus result from a temporal accumulation of the mechanical and thermal strain components [17]. C_{ijkl} is the elasticity tensor of the fourth stage. $\alpha_{th,kl}$ is a tensor describing the linear thermal expansion, and $\xi\left(t\right)$ is a time-scale given by [2]

$$\xi\left(t\right):=\int_0^t\frac{1}{a_T}\,\mathrm{d}t'.$$

3 NUMERICAL SIMULATION OF A FILLING PROCESS

Let us now have a closer look at the numerical simulation of a representative filling process in a thin-walled rectangular channel cavity, as depicted in figure 6. As polymer filling material Hostalen GC 7260 (PE-HD) from LyondellBasell Industries with all relevant material parameters is considered. The walls of the cavity as modelled isothermally with a constant temperature of $T = 308{,}15\,\mathrm{K}$ $(35\,^{\circ}\mathrm{C})$. For the spatial discretization as well as the CFD analysis a structered mesh is build up in ANSYS CFX. For the semi-volumetric model a finite element surface mesh (triangular elements) with networks of bar elements in Cadmould 3D-F.

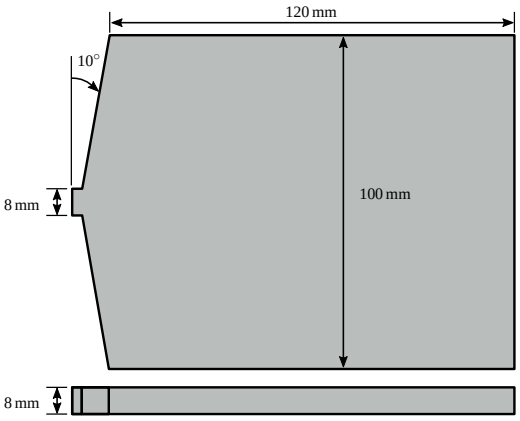

Figure 6: Sketch of the investigated cavity geometry.

The relevant material parameters for the employed Carreau-WLF viscosity model are provided in table 1.
The definition of boundary conditions in ANSYS CFX is straight forward, where it is crucial to prescribe a free slip wall for the air, otherwise the calculation will not converge and air will be trapped at the walls, cf. [6]. The mass flow rate is given as a linear function of time to improve numerical stability. In Cadmould 3D-F the walls are automatically set as no-slip walls and we had to define a short hot runner to guarantee a two-dimensional inlet geometry.

Table 1: Carreau-WLF parameters

parameter	value
A	$589{,}181\,\mathrm{Pa\,s}$
B	$0{,}0136206\,\mathrm{s}$
C	0,50037
T_0	$240\,^{\circ}\mathrm{C}$
T_S	$-68{,}19\,^{\circ}\mathrm{C}$
C_1	8,86
C_2	101,6

Instead of mass flow rate, we had to prescribe an equivalent volume flow rate as function of time. The basic geometry preparation and the generation of a high-quality structured mesh for the CFD simulation in ANSYS CFX was done with ICEM/CFD. In Cadmould 3D-F, an internal CAD toolbox and an internal mesh generator are used. Both models are illustrated in figure 7.

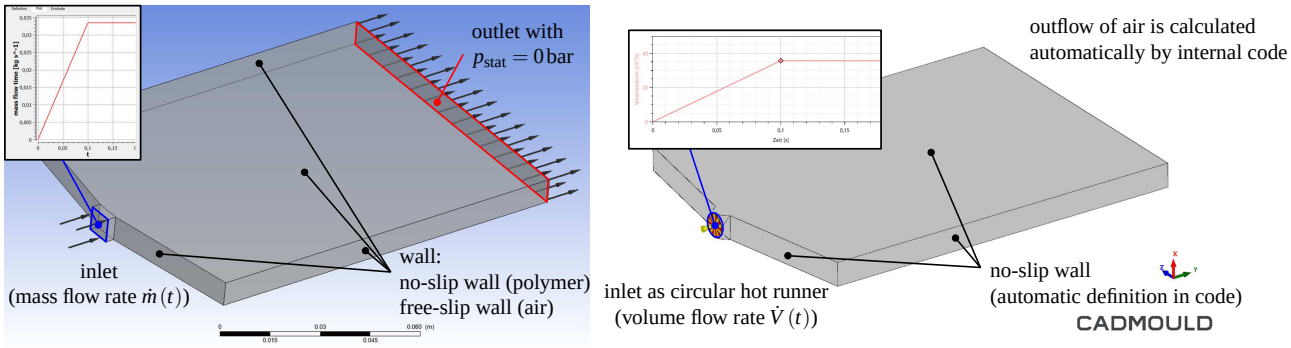

Figure 7: CFD models in ANSYS (left) and Cadmould 3D-F (right).

4 SIMULATION RESULTS

In the simulation results, it can be seen that during the initial filling stage the flow front evolution is characterized by the inflow process of the polymer melt and effects from the inlet geometry as shown in figure 8. In the ANSYS results light eddies at the flow front can be seen as result from the entry flow at the sharp edges. In Cadmould 3D-F results the flow front is more smooth due to the 2,5 dimensional approach.

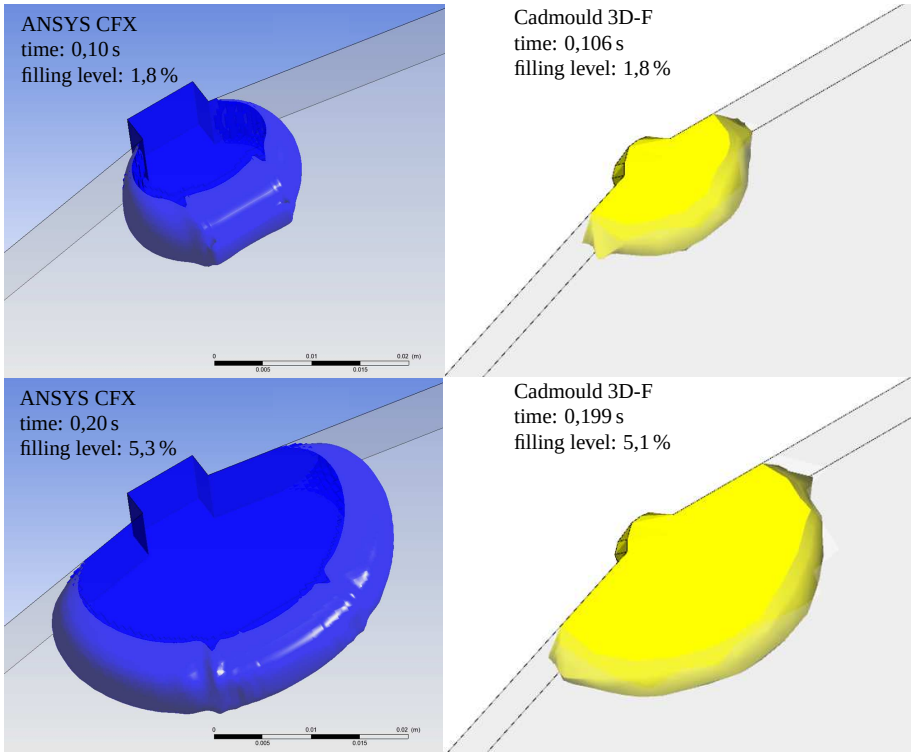

Figure 8: Simulation results for the early filling stages.

During the subsequent filling stages, the polymer melt reaches the side walls of the cavity and then the evolution of a more stretched flow front can be observed as shown in figures 9 and 10. Later, a constant flow front propagation evolves without further deformation of the flow front topology, see figure 11.

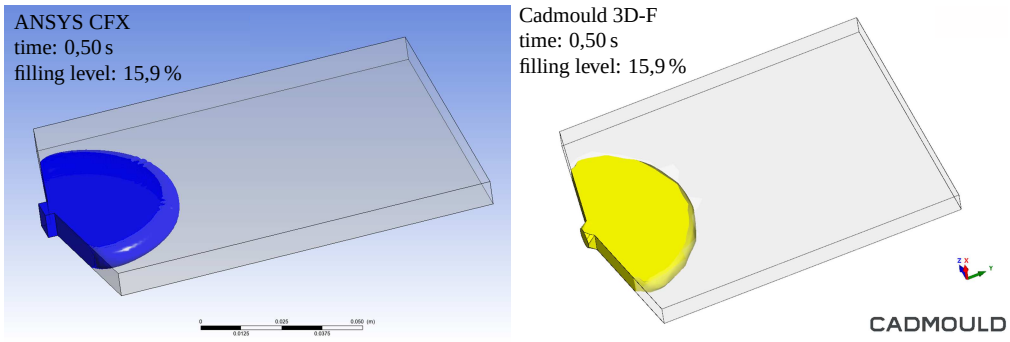

Figure 9: Simulation results for intermediate filling stages.

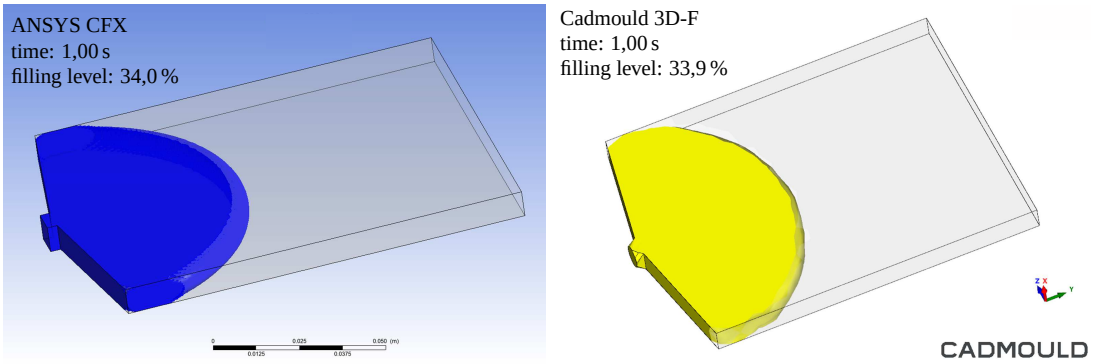

Figure 10: Simulation results for subsequent filling stages.

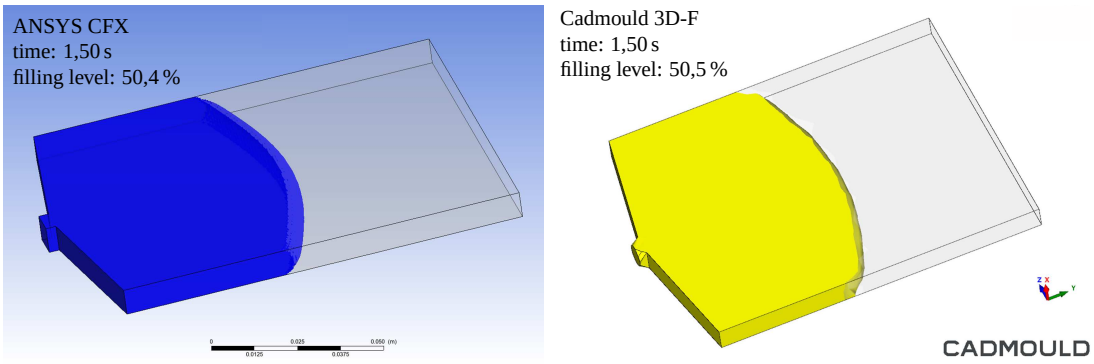

Figure 11: Simulation results for later filling stages.

Finally, a shape analysis of the flow front within the mid-plane of the cavity shows good agreement between the two simulation strategies, cf. figure 12.

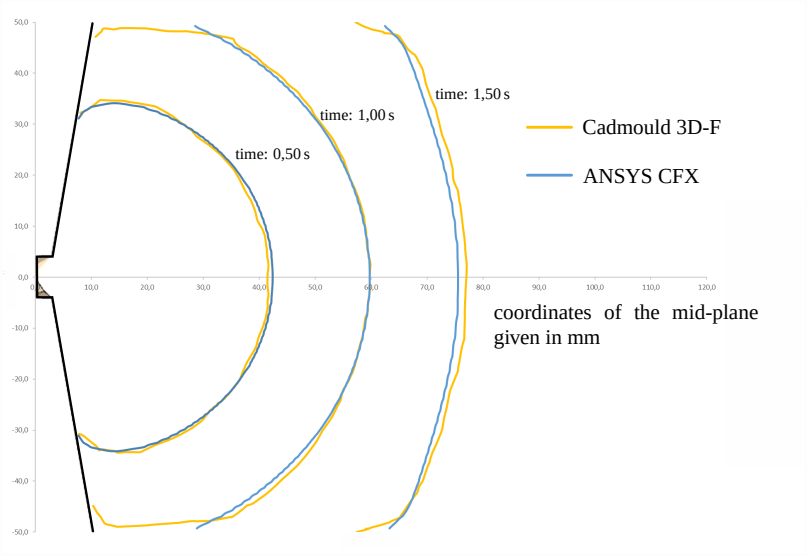

Figure 12: Temporal evolution of the flow front within the mid-plane of the cavity.

5 CONCLUSION AND OUTLOOK

In this contribution, it was demonstrated that the Hele-Shaw approximation employed in the Cadmould 3D-F framework is well suited for sufficiently accurate and efficient simulation of thin-walled structures. Furthermore, there is quite a good agreement between the simulation results of the 3D volumetric model in ANSYS CFX and and the 2,5D semi-volumetric Cadmould 3D-F. Only in the contact area between the side walls and the polymer melt slight differences are observed. The reason for this can be found in the different characterization of the flow front. In 3D approaches the fountain flow regime in the flow front is captured where in the 2.5D approach this effect is neglected. For future studies the authors plan to make further validation of the simulation results with experimental filling studies within the next steps.

6 ACKNOWLEDGEMENTS

This contribution has been developed in the scope of the project OptiTemp. The associated research project OptiTemp (reference number 13FH012PX8) is partly funded by the German Federal Ministry of Education and Research (BMBF) within the research programme FHprofUnt 2018.

REFERENCES

[1] Guevara-Morales, A. and Figueroa-Lopez, U. Residual stresses in injection molded products. *J. Mater. Sci.*, (2014) **49**:4399–4415.

[2] Fernandez, C., Pontes, A. J., Viana, J. C. and Gaspar-Cunha, A. Modelling and optimization of the injection-molding process: a review. *Adv. Polymer Techn.*, (2018) **37**:429–449.

[3] Studer, M. and Ehring, F. Minimization of warpage of injection-molded parts through ideal wall thickness distribution – a feasibility study, *Journal of Plastics Technology*, (2013) **9**:209–252.

[4] Osswald, T.A. and Rudolph, N., *Polymer rheology: fundamentals and applications*. Hanser Publications, (2015).

[5] Simcon Kunststoff-technische Software GmbH, Simulation of fluid flow and structural analysis within thin walled three dimensional geometries. *European Patent Application*. EP 1385103 A1, (2004).

[6] Mukras, S. M. S. and Al-Mufadi, F. A. Simulation of HDPE Mold Filling in the Injection Molding Process with Comparison to Experiments. *Arabian Journal for Science and Engineering*, (2016) **41**:2847–2856.

[7] Zhang, J., Yin, X., Liu, F. and Yang, P. The simulation of the warpage rule of the thin-walled part of polypropylene composite based on the coupling effect of mold deformation and injection molding process. *Science and Engineering of Composite Materials*, (2016) **25**:593–601.

[8] Rusdi, M. S., Abdullah, M. Z., Mahmud, A. S., et al. Numerical Investigation on the Effect of Injection Pressure on Melt Front Pressure and Velocity Drop. *Applied Mechanics and Material*, (2014) **786**:210–214.

[9] Cardozo, D. A brief history of the filling simulation of injection moulding. *Proc. IMechE, J. Mechanical Engineering Science*, (2009) **223**:711–721.

[10] Hieber, C. A. and Shen, S. F. A Finite-Element-Finite-Difference Simulation of the Injection Mold-

ing Filling Process. *Journal of Non-Newtonian Fluid Mechanics*, (1980) **7**:1–32.

[11] Hele-Shaw, H. S. The Motion of a Perfect Liquid. *Proceedings of the Royal Institution of Great Britain*, (1899) **16**:49–64.

[12] Karrenberg, G., Neubrech, B. and Wortberg, J. CFD simulation of plastics plasticizing in an extruder with a continuously grooved cylinde and barrier screw. *Journal of Plastics Technology*, (2013) **12**:205–238.

[13] Nielsen, L. E. and Landel, R. F. *Mechanical Properties of Polymers and Composites*. Marcel Dekker Inc., (1994).

[14] Chiang, H. H., Hieber, C. A. and Wang, K. K. A Unified Simulation of the Filling and Postfilling Stages in Injection Molding. Part I: Formulation. *Polymer Engineering and Science*, (1991) **31**:116–124.

[15] Matin, I., Hadžistević, M., Vukelic, D., et al. Application of numerical simulation of injection molding of medical accessory. *Journal for Technology of Plasticity*, (2016) **41**:47–54.

[16] Rezayat, M., Stafford, R. O. A thermoviscoelastic model for residual stress in injection molded thermoplastics. *Polymer Engineering and Science*, (1991) **31**:393–398.

[17] Studer, M. and Ehring, F. Minimizing Part Warpage in Injection Molding by Optimizing Wall Thickness Distribution, *Advances in Polymer Technology*, (2014) **33**:21454.